Temperature Dependence of Molecular Conformation, Dynamics, and Chemical Shift Anisotropy of α,α-Trehalose in D_2O by NMR Relaxation

Gyula Batta,*,†,§ Katalin E. Kövér,‡ Jacquelyn Gervay,† Miklós Hornyák,§ and Gareth M. Roberts†

Contribution from the Department of Chemistry, The University of Arizona, Tucson, Arizona 85721, NMR Laboratory, L. Kossuth University, H-4010 Debrecen, Hungary, and Research Group for Antibiotics, Hungarian Academy of Sciences, L. Kossuth University, H-4010 Debrecen, P.O. Box 70, Hungary

Received August 12, 1996[⊗]

Abstract: A molecular dynamics study and solution-phase ^{1}H and ^{13}C chemical shift anisotropy determination of a symmetric cryogenic disaccharide, α,α-trehalose, has been performed in a temperature range between 264 and 350 K. Negligible temperature dependence of proton−carbon couplings of the asymmetrically [1-^{13}C]-labeled trehalose suggest that the averaged conformation of the interglycosidic linkage is centered around dihedral angles $\phi = \psi = -41°$ with ±5° uncertainty. Homonuclear NOE-s in the labeled trehalose support the dominance of similar conformation. Close to the slow and fast motional regime, α,α-trehalose can be considered as a spherical top, and global correlation times can be determined easily at extreme temperatures. This allows the construction of an Arrhenius plot for the whole range of temperature. The approach, which we call "trouble-free", yields $E_a = 28.2$ kJ/mol for the activation energy of molecular reorientation. The model-free analysis of ^{13}C T_1, T_2, and NOE data showed a local maximum of the generalized order parameters with $S^2 = 0.9$ around 273 K. Monte-Carlo error analysis corroborated that this effect could be real; however, effective correlation times have relatively high error limits. Thermodynamically, the S^2 data can be interpreted in terms of changes in the Gibbs free energy due to increased or diminished spatial restriction of rapid CH fluctuations. Liquid state ^{1}H and ^{13}C chemical shift anisotropies were determined from the interference of dipole−dipole and chemical shift anisotropy relaxation. In solution, chemical shift anisotropies cannot be separated from an inherent geometrical factor, so a combined CSA_g factor was used. Cross-correlated spectral densities could be well fitted for the C-1,H-1 vector over the entire temperature range with the "trouble-free" global correlation times. The resulting numerical values for CSA_g were smaller compared to the model-free evaluation, due to the omission of internal fluctuations. The measured shift anisotropies were found to be independent from the selection of isotropic or anisotropic dynamical models. Apparent CSA_g factors were nearly constant in the entire temperature range except C-3, H-2, and H-3. Comparison with deuterium labeled [2,4,6-^{2}H]-trehalose proved that temperature-induced changes of the ABX-type strong coupling pattern (caused by the change of differential chemical shift of vicinal H-2 and H-3 protons) interfere with asymmetric multiplet relaxation and potentially lead to misinterpretation of CSA/DD relaxation rates.

Introduction

α,α-Trehalose **1** is a symmetric α-(1−1) linked nonreducing disaccharide of glucose, a dominant isomer of trehalose in nature. It is found in high concentrations in organisms which are able to survive complete dehydration and is also a cryoprotectant against the freeze-drying cycle.[1] Two distinct phenomena may be at play in both of these functions.[2] Dehydration can cause structural damage to the membrane which in turn causes functional defects. One hypothesis is that trehalose replaces the hydrogen bonding interactions normally present in hydrated biomembranes, allowing dehydration to occur without subsequent membrane damage.[3] The cryoprotectant qualities of trehalose may be more closely associated with its ability to organize surrounding water molecules in a manner which maximizes apolar interactions and stabilizes the bilayer structure.[4] Differential scanning calorimetry and ^{17}O relaxation studies indicate that trehalose has the highest relative number of unfrozen coordinated water molecules when compared to other cryoprotective sugars such as sucrose and maltose.[4]

The conformational features of trehaloses are supported by optical rotation[5] ($\phi = \psi = -60°$), X-ray crystallographic studies[6] (−41°, −58° for the dihydrate and −60°, −59° for the anhydrous form), and MM3 (−44°, −44°) or MM2CARB (−55°, −55°) molecular mechanics calculations.[7] The calculations suggest that α,α-trehalose exists predominantly in one preferred conformation in solution. Until now, symmetry of

† The University of Arizona.

‡ NMR Laboratory, L. Kossuth University.

§ Hungarian Academy of Sciences, L. Kossuth University. Permanent address (G.B.) for correspondence.

⊗ Abstract published in *Advance ACS Abstracts,* January 15, 1997.

(1) Nakagaki, M.; Nagase, H.; Ueda, H. *J. Membr. Sci.* **1992**, *73*, 173−180.

(2) Crowe, J. H.; Carpenter, J. F.; Crowe, L. M.; Anchordoguy, T. J. *Cryobiology* **1990**, *27*, 219.

(3) Crowe, J. H.; Crowe, L. M.; Chapman, D. *Science* **1984**, *223*, 701.

(4) Kawai, H.; Sakurai, M.; Inoue, Y.; Chujo, R.; Kobayashi, S. *Cryobiology* **1992**, *29*, 599−606.

(5) Duda, C. A.; Stevens, E. S. *J. Am. Chem. Soc.* **1990**, *112*, 7406. Duda, C. A.; Stevens, E. S. *J. Am. Chem. Soc.* **1993**, *115*, 8487.

(6) (a) Brown, G. M.; Rohrer, D. C.; Berking, B.; Beevers, C. A.; Gould, R. O.; Simpson, R. *Acta Crystallogr.* **1972**, *B28*, 3145. (b) Jeffrey, G. A.; Nanni, R. *Carbohydr. Res.* **1985**, *137*, 21−30.

(7) (a) Dowd, M. K.; Reilly, P. J.; French, A. D. *J. Comput. Chem.* **1992**, *13*, 102. (b) Tvaroska, I.; Vaclavik, L. *Carbohydr. Res.* **1987**, *160*, 137−149. In ref 7b calculations were carried out with 2-(tetrahydropyran-2-yloxy)tetrahydropyran which is closely related to trehalose.

S0002-7863(96)02807-7 CCC: $14.00

α,α-trehalose did not allow detailed NMR studies concerning the conformation of its glycosidic linkage.

The stability of the average conformation about the glycosidic linkage was investigated using asymmetrically [1-^{13}C]-labeled trehalose, through the measurement of heteronuclear interglycosidic coupling constants over a broad temperature range. A further consideration was whether fast internal fluctuations might impact upon the cryogenic behavior of trehalose. If water molecules are strongly coordinated[4] to their disaccharide host, then internal fluctuations of the host may spread to the hydration shell and vice versa, and possibly affect the freezing point of the solution. This work presents a temperature-dependent molecular dynamics and chemical shift anisotropy study of trehalose to explore this hypothesis. Since solution phase chemical shift anisotropies may be sensitive to solvation effects and OH rotamer populations, we measured the proton and carbon chemical shift anisotropy as a function of temperature.

It has recently been shown that ^{1}H and ^{13}C chemical shift anisotropy factors (CSA_g)[8] can be determined from concentrated aqueous solutions of carbohydrates at *natural abundance*. The determination of anisotropy parameters is inherently connected to molecular dynamics, therefore we extend our CSA_g method to include the isotropic and anisotropic forms of the model-free approach of NMR molecular dynamics.[9−11] Here we also make a comparison of three different dynamical approaches to select the best for monitoring the CSA_g term in a wide temperature range.

Theory

Chemical Shift Anisotropy in Solution. Chemical shift anisotropy is generally not manifested in isotropic liquids because the principal components of the chemical shift tensor average to a scalar quantity. However, field dependency of relaxation rates or interference effects (cross-correlated relaxation causes differential multiplet relaxation or line broadening) between different mechanisms of relaxation may report on CSA.

Excellent papers and reviews[12] were recently published on longitudinal and transversal scalar coupled relaxation of half-spin nuclei. In this work we confine studies to the longitudinal relaxation of CH groups, which is appropriate for most carbohydrate studies, and in practice we implement the initial rate two-spin approach.[13] In order for this approach to be justified the contribution of inter- and intramolecular proton relaxation to the measured cross-correlated spectral densities must be negligible. Grant et al. has shown that the initial rate is free from these complications in the case of ethanol.[14] The intermolecular proton relaxation effects can be handled as external random-field terms[14,15] and omission of long-range intramolecular proton interactions does not lead to serious errors in a full relaxation treatment. These results encourage the application of an initial-rate two-spin approach for extraction of DD/CSA cross-correlated spectral densities for carbohydrates. There are more sophisticated approaches to obtain interference terms in relaxation experiments.[16,17]

Here, we are going to demonstrate the potential of a simple and sensitive method[8] for measuring ^{1}H and ^{13}C CSA data in solution. This method may roughly be divided into two separate steps. First, the DD/CSA cross-correlated spectral densities are measured from the initial slope of longitudinal relaxation experiments, where interconversion of $\langle 2S_zI_z\rangle$ magnetization to and from $\langle I_z\rangle$ or $\langle S_z\rangle$ is detected. Second, the molecular dynamics are characterized by a simple method we call "trouble-free" or by the well-known model-free method of Lipari and Szabo. Finally, combination of the dynamics and cross-correlated relaxation yields the chemical shift anisotropy terms.

Conventionally, for an IS two-spin system (I = ^{13}C, S = ^{1}H), the equation of motion of longitudinal magnetizations is given in the form of generalized Solomon equations (eq 1).

$$\mathrm{d}(\boldsymbol{\nu})/\mathrm{d}t = -\mathbf{R}\boldsymbol{\nu}(t) \tag{1}$$

where

$$\boldsymbol{\nu} = \begin{matrix}\langle \Delta S_z\rangle \\ \langle \Delta I_z\rangle \\ \langle 2S_zI_z\rangle\end{matrix} \quad \text{and} \quad \mathbf{R} = \begin{matrix}\rho_S & \sigma_{IS} & \delta_{SIS} \\ \sigma_{IS} & \rho_I & \delta_{SII} \\ \delta_{SIS} & \delta_{SII} & \rho_{IS}\end{matrix}$$

The relaxation matrix **R** contains diagonal elements ρ which are the intrinsic relaxation rates, the σ terms are the cross-relaxation rates due to dipole−dipole interactions, and the δ terms are the cross-correlated relaxation rates arising from the interference between the DD and CSA mechanisms of relaxation. It follows from the solution of eq 1 that the cross-correlated relaxation rate in the initial rate approach is given as shown in eq 2.[13] Where $\langle 2S_zI_z\rangle$ is the amount of two-spin order after a short period of time dt and $\langle S_z^0\rangle$ is the equilibrium magnetization of the inverted spin S.

$$\delta_{SIS} = \langle 2S_zI_z\rangle/(2\langle S_z^0\rangle\,\mathrm{d}t) \tag{2}$$

The measured δ_{SIS} rates are directly proportional to the appropriate spectral densities as shown by eq 3.

$$\delta_{SIS} = -4J_{SIS}(\omega_S) \tag{3}$$

For determination of the cross term δ_{SIS} Farrar et al.[12t] proposed a two-spin approach based on Redfield's theory. In their isotropic model they considered the external random field contributions of both the protons and the heteronuclei and

(8) Batta, Gy.; Gervay, J. *J. Am. Chem. Soc.* **1995**, *117*, 368−374.
(9) Lipari, G.; Szabo, A. *J. Am. Chem. Soc.* **1982**, *104*, 4546. Lipari, G.; Szabo, A. *J. Am. Chem. Soc.* **1982**, *104*, 4559.
(10) Dellwo, M. J.; Wand, J. *J. Am. Chem. Soc.* **1989**, *111*, 4571.
(11) Brüschweiler, R.; Case, D. A. *Prog. NMR Spectrosc.* **1994**, *26*, 27.
(12) (a) Shimizu, H. J. *J. Chem. Phys.* **1964**, *40*, 3357. (b) Mackor, E. L.; Maclean, C. *J. Chem. Phys.* **1966**, *44*, 64. (c) Werbelow, L. G.; Grant, D. M. *Adv. Magn. Reson.* **1977**, *9*, 189. (d) Vold, R. L.; Vold, R. R. *Prog. NMR Spectrosc.* **1978**, *12*, 79. (e) Guéron, M.; Leroy, J. L.; Griffey, R. H. *J. Am. Chem. Soc.* **1983**, *105*, 7262. (f) Keeler, J.; Sánchez-Ferrando *J. Magn. Reson.* **1987**, *75*, 96. (g) Canet, D. *Prog. NMR Spectrosc.* **1989**, *21*, 237. (h) Oschkinat, H.; Bermel, W. *J. Magn. Reson.* **1989**, *81*, 220. (i) Dalvit, C.; Bodenhausen, G. *Chem. Phys. Lett.* **1989**, *161*, 554. (j) Liu, F.; Mayne, C. L.; Grant, D. M. *J. Magn. Reson.* **1989**, *84*, 344. (k) Boyd, J.; Hommel, U.; Campbell, I. D. *Chem. Phys. Lett.* **1990**, *175*, 477. (l) Chang, W.-T.; Wang, P.-L.; Duh, D.-M.; Hwang, L.-P. *J. Phys. Chem.* **1990**, *94*, 1343. (m) Di Bari, L.; Kowalewski, J.; Bodenhausen, G. *J. Chem. Phys.* **1990**, *93*, 7698. (n) Werbelow, L. *J. Phys. Chem.* **1990**, *94*, 6663. Dalvit, C. *J. Magn. Reson.* **1991**, *95*, 410. (o) Grant, D. M.; Mayne, C. L.; Liu, F.; Xiang, T. X. *Chem. Rev.* **1991**, *91*, 1591. (p) Farrar, T. C.; Jablonsky, J. *J. Phys. Chem.* **1991**, *95*, 9159. (q) Kontaxis, G.; Muller, N.; Sterk, H. *J. Magn. Reson.* **1991**, *92*, 332. (r) Tsai, C.-L.; Price, W. S.; Chang, Y.-C.; Perng, B.-C.; Hwang, L.-P. *J. Phys. Chem.* **1991**, *95*, 7546. (s) Maler, L.; Kowalewski, *J. Chem. Phys. Lett.* **1992**, *192*, 595. (t) Trudeau, J. D.; Bohmann, J.; Farrar, T. C. *J. Magn. Reson. Ser. A* **1993**, *105*, 151. (u) Brown, R. A.; Grant, D. M. *J. Magn. Reson. Ser. A* **1993**, *105*, 284. (v) Poppe, L.; van Halbeek, H. *Magn. Reson. Chem.* **1993**, *31*, 665. (w) Maler, L.; Di Bari, L.; Kowalewski, J. *J. Phys. Chem.* **1994**, *98*, 6244.
(13) Jaccard, G.; Wimperis, S.; Bodenhausen, G. *Chem. Phys. Lett.* **1987**, *138*, 601.
(14) Zheng, Z.; Mayne, C. L.; Grant, D. M. *J. Magn. Reson. Ser. A* **1993**, *103*, 268. It was demonstrated that in the initial rate period, the magnetization buildup curves were indistinguishable from those where deuterium substitution was applied at protons adjacent to the CH_2 group. This is not surprising as buildup of multispin effects generally takes longer time for dipolarly coupled spins.
(15) Fuson, M. M.; Belu, A. M. *J. Magn. Reson. Ser. A* **1994**, *107*, 1.
(16) Bremi, T.; Ernst, M.; Ernst, R. R. *J. Phys. Chem.* **1994**, *98*, 9322−9334.
(17) (a) Levitt, M. H.; DiBari, L. *Phys. Rev. Lett.* **1992**, *69*, 3124. (b) Levitt, M. H.; DiBari, L. *Bull. Magn. Reson.* **1993**, *16*, 94.

successfully simulated experiments differing in preparation of the spin system.

For the purposes of this work we assume an axially symmetric chemical shift tensor and the angle subtended by the tensor axis and the CH vector is defined as ϕ_{SIS}.[18] Equation 4 shows that the cross-correlated spectral density is linearly dependent on the external magnetic field B_o and the shielding anisotropy $\Delta\sigma_S$. (Where S and I indices are interchangeable although S normally refers to ^{1}H and I to ^{13}C.) The $J(\omega_S,\tau_C)$ spectral densities vary according to the selected dynamical approach. If a molecule tumbles isotropically and rapid intramolecular fluctuations are omitted, eq 5 may be applied.

$$J_{SIS}(\omega_S) = (\mu_o/16\pi)\,\gamma_S{}^2\gamma_I\,(h/2\pi)\,\langle r_{IS}{}^{-3}\rangle B_o\Delta\sigma_S J(\omega_S,\tau_C) \times \{0.5(3\cos^2\phi_{SIS} - 1)\} \quad (4)$$

$$J(\omega_S,\tau_C) = 0.4\tau_C/(1 + \omega_S{}^2\tau_C{}^2) \quad (5)$$

Since the shift anisotropy and the geometric term of eq 4 are not separable in solution we use a combined, geometry dependent chemical shift anisotropy (CSA_g) factor[8] that is derived from eq 4 by setting $\phi_{SIS} = 0$, and reversing the sign (a change from shielding to chemical shift anisotropy in ppm units).

$$CSA_g = -16\pi\, J_{SIS}(\omega_S)[\mu_o B_o\gamma_S{}^2\gamma_I(h/2\pi)\langle r_{IS}{}^{-3}\rangle\, J(\omega_S,\tau_C)]^{-1}(10^6) \quad (6)$$

By this definition, the convention for CSA_g gives a lower limit for the absolute value of the CSA; however, it should be a sensitive indicator of changes either in the orientation or in the anisotropy of the chemical shift tensor.

Molecular Dynamics. If we wish to use simple molecular dynamics described by a single, isotropic rotational correlation time, the spectral density function of eq 5 may be used. Due to the dipolar coupling between directly bonded ^{13}C and ^{1}H nuclei, the heteronuclear cross-relaxation rates σ_{IS} can be determined from steady-state ^{13}C−{^{1}H} NOE difference (NOEF) and ^{13}C T_1 relaxation time under broad-band ^{1}H decoupling.

$$\sigma_{IS} = \gamma_I\mathrm{NOEF}/(\gamma_S T_1) \quad (7)$$

This rate can be measured accurately, as both the NOEF and the T_1 are proportionally decreased by concurrent relaxation channels (e.g. CSA). The cross-relaxation rate depends on the spectral densities at zero and double-quantum frequencies, hence τ_C can be back calculated from the measured σ_{IS}.

$$\sigma_{IS} = 0.1K^2\tau_C\{6/(1 + (\omega_I + \omega_S)^2\tau_C{}^2) - 1/(1 + (\omega_I - \omega_S)^2\tau_C{}^2)\} \quad (8)$$

$$K = (\mu_o/4\pi)\gamma_S\gamma_I(h/2\pi)r_{IS}{}^{-3}$$

For carbohydrates an average CH bond distance of $r_{IS} = 0.112$ nm is accepted.[19] The $\sigma_{IS}(\tau_C)$ function is not unequivocal, and generally gives two solutions for τ_C. Only toward the extreme narrowing or the extreme broadening regime are the two solutions well separated and distinguishable. It should be noted that the cross-relaxation rate σ_{IS} is also available from the initial buildup rate of the transient NOE; however, in practice the transient method is less accurate.

In the isotropic form of the model-free approach[9] (eq 9) the spectral density includes parameters for local fluctuations and ordering.

$$J(\omega_S,\tau_C) = 0.4\{S^2\tau_C/(1 + \omega_S{}^2\tau_C{}^2) + \tau(1 - S^2)/(1 + \omega_S{}^2\tau^2)\} \quad (9)$$

$$\tau^{-1} = \tau_C{}^{-1} + \tau_e{}^{-1}$$

Here τ_C represents the global correlation time for molecular reorientation, and the S^2 generalized order parameters show the extent of spatial restriction of local motions. The τ_e effective correlation times describe fast local fluctuations of CH vectors. Lipari and Szabo extended their formalism for the case of anisotropic reorientation and introduced two different global correlation times τ_1 and τ_2, and an asymmetry parameter A (see Supporting Information). There are other extensions[20] of the model-free approach that are relevant to more complicated motional behavior and they will not be considered in this work.

If the carbons in a molecule relax exclusively through the dipolar interaction of their attached protons, then the measurable ^{13}C relaxation data can be given theoretically.[9] The dynamical data can be obtained if we fit T_1 and NOEF data at two different magnetic fields or T_1, T_2, and NOEF at a single field. It is known that methine ^{13}C chemical shift anisotropy is moderate in carbohydrates (30−40 ppm).[18,21] Consequently, the CSA contribution to carbon intrinsic relaxation is less then 4% at the highest applied field (11.7 T). Since the actual CSA values are not known *a priori*, it is probably better to neglect their contribution from the dynamical calculations. However, cross-correlated relaxation effects can and must be suppressed with suitable experimental techniques.

Results and Discussion

Conformation of Trehalose. Earlier NMR results[22] showed that the glucopyranoside rings in trehalose are in a $^4C_1$ conformation. The conformation of the glycosidic linkage (dihedral angle H1−C1−O−C1′) in related unsymmetrical disaccharides was estimated as $\Phi = \Psi = -50 \pm 10°$ from homonuclear NOE data and heteronuclear couplings. The dihedral angle is difficult to measure without labeling since line broadening at high concentration obscures small long-range couplings. Furthermore, chemical equivalence in trehalose makes interglycosidic ^{1}H−{^{1}H} NOE factors unavailable. To circumvent these difficulties we synthesized the asymmetrically labeled [1-^{13}C]trehalose. One- and two-dimensional NOE experiments were run at 500 MHz to reveal interglycosidic contacts through space. Though rotational correlation times from ^{13}C T_1 and heteronuclear NOE were found to be close to extreme narrowing for a dilute solution (ca. 100 ps at room temperature for a ca. 20 mg/mL concentration), the NOE between the anomeric protons was unusually small. The H1*−{H1}[23] NOE was only +2.6%, which is significantly smaller than the intraunit H2−{H1} NOE of ca. +10%. This is

(18) Sherwood, M. H.; Alderman, D. W.; Grant, D. M. *J. Magn. Reson. Ser. A* **1993**, *104*, 132. It is well established for carbohydrates that for a carbon bonded to an oxygen, the orientation of the δ_{33} principal axis is nearly parallel to the C−O bond, and the two other perpendicular principal values are shifted downfield by ca. 30−40 ppm. The axis assigned as Y declines from the CH bond by ca. 20°, and it has the highest principal value around 90 ppm. In accordance with solid state data, our preliminary results obtained by the comparison of Grant's solid state and our liquid state CSA data show that the "quasi" axis of the carbon shift tensors with respect to the CH bond in sucrose and Me α-D-glucopyranoside may be in between 10° and 35°.

(19) McCain, D. C.; Markley *J. Am. Chem. Soc.* **1986**, *108*, 4259.

(20) (a) Clore, M. G.; Szabo, A.; Bax, A.; Kay, L. E.; Driscoll, P. C.; Gronenborn, A. M. *J. Am. Chem. Soc.* **1990**, *112*, 4989−4991. (b) Barbato, G.; Ikura, M.; Kay, L. E.; Pastor, R. W.; Bax, A. *Biochemistry* **1992**, *31*, 5269−5278.

(21) Hricovini, M.; Torri, G. *Carbohydr. Res.* **1995**, *268*, 159−175.

(22) Bock, K.; Defaye, J.; Driguez, H.; Bar-Guilloux, E. *Eur. J. Biochem.* **1983**, *131*, 595.

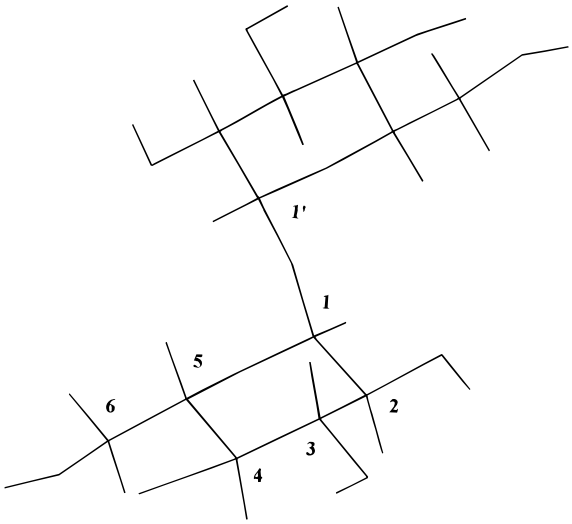

Figure 1. Minimum energy conformation of α,α-D-trehalose as given by MM3 molecular mechanics. Interglycosidic dihedral angles are identical; $\phi = \psi = -44°$.

surprising at first glance since according to MM3 calculations the two distances in the preferred conformation (Figure 1) are nearly identical, i.e. 0.27 and 0.25 nm. To rule out accidental spill-over effects, the 2D NOESY experiment ($\tau_{mix} = 400$ ms) was also evaluated. Again, the intraunit effect was at least four times stronger (Figure 2).[24] The weak NOE between the anomeric protons can be explained by an indirect $^1H \rightarrow {}^{13}C \rightarrow {}^1H$ NOE pathway caused by the [1-^{13}C] label. For the given geometry ($r_{H1-H1*} = 0.27$ nm, $r_{H1*-C1*} = 0.112$ nm, $r_{H1-C1*} = 0.26$ nm) the theoretical maximum (50%) of the H1*−{H1} homonuclear NOE cannot be bigger than 5% because of the indirect effect.[25] Consequently, a strong 25% interglycosidic NOE would reduce to ca. +2.5%, which is close to our experimental result. The ca. +10% NOE from H1 to the overlapping H3,H5,H5* region corroborates the MM3 predicted 0.3 nm H1−H5* interglycosidic distance, since the intraunit H1−H3 and H1−H5 distances are close to 0.4 nm, and cannot significantly contribute to the measured enhancement. Steady state NOE experiments at low field (200 MHz) provided an identical (+2.5%) interanomeric NOE value. However, the intraunit H2−{H1} NOE increased from +10% to +13−14%. This modest difference in field dependency is not informative about the rigidity of the glycosidic bond. A selective heteronuclear NOE experiment yielded a small (−1%) negative heteronuclear three-spin effect at the labeled carbon, when the H1 attached to ^{12}C-1 was saturated, as shown in a previous study at natural abundance.[26] In summary, the semiquantitative interpretation of the homonuclear NOE's in the asymmetrically ^{13}C labeled trehalose supports the preferred conformation suggested by MM3 molecular mechanics. However, the accuracy of NOE's is insufficient for a clear selection between theoretical models.

The interglycosidic bond angle was measured from the resolved $^3J_{H1,C,O,^{13}C1}$ coupling constant. Since no other resolved long-range coupling was detected, simple proton-coupled carbon spectra provided the coupling constant. From 86 independent measurements at different temperatures between 272 and 350 K the heteronuclear coupling was found to be 3.3 ± 0.5 Hz with 90% confidence. This translates to dihedral angle $\Phi = \Psi = -41 \pm 5°$, if we accept the parameters of a Karplus curve published recently,[27,28] and is different from the anhydrous crystal structure.[6b] Theoretical MM3 calculation[7] predicts one dominant conformer for α,α-trehalose with angles $\Phi = \Psi = -44°$. Moreover, it was stated that "since the energy of global minimum is several kcal/mol lower than that of the other two minima, the dominant conformer present in solution predicted by modeling should be the same as that in vacuo." Indeed, our NMR experiments strongly suggest that the interglycosidic conformation of α,α-trehalose is probably less flexible than most related disaccharides. However, librational motions of glucopyranose rings, perhaps, may play a role in its dynamical behavior.

Temperature-Dependent Molecular Dynamics. There is a growing interest in exploring the molecular dynamics of saccharides[29,30] and there are contradictory results about the rigidity of the glycosidic bond in oligosaccharides.[31] Recent advances in molecular dynamics calculations[32] allow tracking of molecular trajectories on a nanosecond time scale and provide a way for the calculation of NMR observables.

Global Reorientation. Although the preferred conformation of trehalose shows remarkable stability, we were concerned about the global and microdynamics of the trehalose as a function of temperature since reliable dynamical parameters are essential for the determination of chemical shift anisotropy in

(23) In solution we had a mixture of single labeled and unlabeled trehalose in a ratio of 53:47 as estimated from the integral of the anomeric ^{1}H signals. The protons at the labeled half of [1-^{13}C]trehalose are identified by asterisks. NOE factors were calculated after appropriate normalization.

(24) It can be shown theoretically, and was found experimentally (H2−{H1*} NOE was also +10%), that the intraunit H2−{H1} NOE is in fact independent from the ^{13}C label. The H1−{H1*} NOE cannot be safely determined since simultaneous irradiation of the ^{13}C split doublet of H1* partially saturates the H1 center lines.

(25) (a) Noggle, J. H.; Schirmer The Nuclear Overhauser Effect−Chemical Applications; Academic Press: New York, 1971. (b) Batta, Gy.; Kövér, K. E.; Mádi, Z. L. *J. Magn. Reson.* **1987**, *73*, 477. (c) Neuhaus, D.; Williamson, M. In *The Nuclear Overhauser Effect in Structural and Conformational Analysis*; VCH Publishers: New York, 1989. In the structurally related [1-^{13}C] Me α-D-glucopyranoside the H2−{H1} NOE was +10% at 200 MHz. (d) Batta, Gy.; Kövér, K. E.; Gervay, J. *J. Magn. Reson. Ser. B* **1994**, *103*, 185−188.

(26) Batta, Gy.; Kövér, K. E. *Magn. Res. Chem.* **1988**, *26*, 852.

(27) Tvaroska, I.; Hricovini, M.; Petrakova, E. *Carbohydr. Res.* **1989**, *189*, 359. Tvaroska, I.; Taravel, R. F. In *Adv. Carbohydr. Chem. Biochem.* **1996**, *51*, 15−57. In fact, the uncertainty range of the interglycosidic dihedral angle is independent from the slight differences in parametrization of the pertinent Karplus curve. However, insufficient experimental data between 30° and 90° dihedral angles in the literature may have caused errors in parametrization and this can bias the mean value. A comparison with concurrent parameter sets showed that an additional ±5° error is possible. In other words, the accuracy of the measured dihedral angles is ca. ±10°, but the scatter caused by temperature changes in this study is within ±5°.

(28) It is possible that the interglycosidic dihedral angle slightly opens (<2°) within this range upon cooling down the solution; however, this could not be proved unequivocally because of the broadening of C1 lines at low temperature.

(29) (a) McCain, D. C.; Markley, J. L. *J. Magn. Reson.* **1987**, *73*, 244. (b) Kovacs, H.; Bagley, S.; Kowalewski, J. *J. Magn. Reson.* **1989**, *85*, 530. (c) van Halbeek, H.; Poppe, L. *Magn. Reson. Chem.* **1992**, *30*, 574. (d) Bagley, S.; Kovacs, H.; Kowalewski, J.; Widmalm, G. *Magn. Reson. Chem.* **1992**, *30*, 733. (e) Roy, R.; Tropper, F. D.; Williams, A. J. *Can. J. Chem.* **1993**, *71*, 1995. (f) Hajduk, P. J.; Horita, D. A.; Lerner, L. E. *J. Am. Chem. Soc.* **1993**, *115*, 9196. (g) Rutherford, T. J.; Partridge, J.; Weller, C. T.; Homans, S. W. *Biochemistry* **1993**, *32*, 12715. (h) Girlich, D.; Ludeman, H.-D. *Z. Naturforsch.* **1993**, *48c*, 407. (i) Kowalewski, J.; Widmalm, G. *J. Phys. Chem.* **1994**, *98*, 28.

(30) Dais, P. In *Adv. Carbohydr. Chem. Biochem.* **1995**, *51*, 63−131.

(31) (a) Hricovini, M.; Shah, R. N.; Carver, J. P. *Biochemistry* **1992**, *31*, 10018. (b) Poppe, L.; van Halbeek, H. *J. Am. Chem. Soc.* **1992**, *114*, 1092.

(32) (a) Hardy, B. J.; Egan, W.; Wildmalm, G. *Int. J. Biol. Macromol.* **1995**, *17*, 149−160. (b) Balling Engelsen, S.; Pérez, S.; Braccini, I.; Hervé du Penhoat, C. *J. Comput. Chem.* **1995**, *16*, 1096−1119. (c) Balling Engelsen, S.; Hervé du Penhoat, C.; Pérez, S. *J. Phys. Chem.* **1995**, *99*, 13334−13351. (d) Bouchemal-Chibani, N.; Braccini, I.; Hervé du Penhoat, C.; Michon, V. *Int. J. Biol. Macromol.* **1995**, *17*, 177−182. (e) André, I.; Mazeau, K.; Taravel, E. F.; Tvaroska, I. *Int. J. Biol. Macromol.* **1995**, *17*, 189−198. (f) Aida, M.; Sugawara, Y.; Oikawa, S.; Umemoto, K. *Int. J. Biol. Macromol.* **1995**, *17*, 227−235. (g) Koca, J.; Pérez, S.; Imberty, A. *J. Comput. Chem.* **1995**, *16*, 296−310.

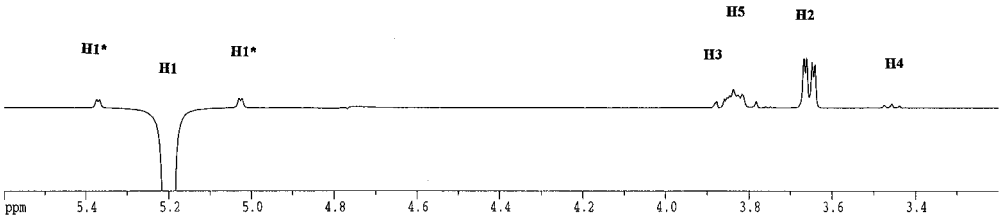

Figure 2. Cross section from a ^{1}H 2D NOESY experiment of a dilute D_2O solution of single-labeled [1-^{13}C]trehalose. The measurement was carried out at room temperature using a DRX 500 spectrometer. The phase sensitive spectrum was obtained with the TPPI method and a mixing time of 0.4 s was allowed. Interanomeric H1···H1* NOE is clearly detected, but it is significantly weaker than the intraunit H1···H2 NOE, due to the effect of the ^{13}C label.

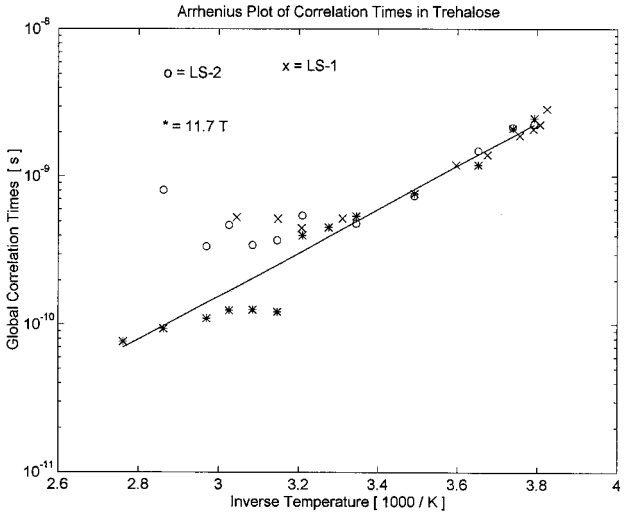

Figure 3. Isotropic global correlation times plotted as a function of inverse temperature on a semilogarithmic scale (Arrhenius plot). The points obtained by the Lipari−Szabo method are labeled with "○", and they were obtained from the combined 5.8 and 11.7 T T_1 and NOE measurements. Points with "×" label represent model free correlation times from T_1, T_2, and NOE values measured at 4.7 T. Correlation times calculated directly from cross-relaxation rates at 11.7 T (eq 7) are labeled with an asterisk. A straight line was obtained from the fit of the four lowest and the two highest points, excluding data between 337 and 287 K. The points of this line represent the "trouble-free" correlation times for the whole region of temperature.

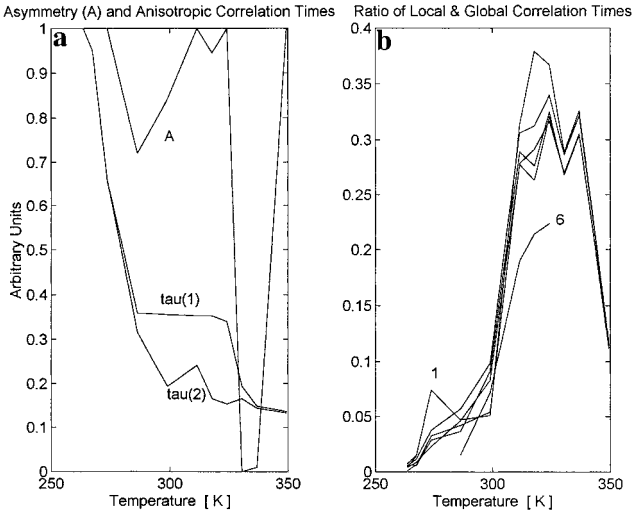

Figure 4. (a) Application of the anisotropic model-free model on the same experimental relaxation data. It can be seen that anisotropic reorientation of trehalose is unlikely below 300 K. Lack of anisotropic reorientation suggests heavy hydration of the disaccharide which is able to compensate against the apparent asymmetry of its dominant conformation (cf. Figure 1). (b) Ratio of local and global correlation times in trehalose as obtained from the application of the isotropic model-free analysis. There is more than one order of magnitude difference between the two time scales below 300 K. Hence, low-temperature data can be safely evaluated. Interpretation of model-free parameters above 300 K may be doubtful.

solution. To this end ^{13}C T_1 and NOEF values were measured with broad-band ^{1}H decoupling at two different magnetic fields. Relaxation data were evaluated in the frame of the "trouble-free" and model-free approaches as described in the theoretical and experimental sections, and are shown in Figure 3. The Arrhenius fit of the global correlation times (11.7 T, eq 7) gives a straight line if we exclude the points in the intermediate temperature range (287 K < T < 349 K) from fitting. Also, the correlation times obtained from cross-relaxation rates at 5.8 T converge to 11.7 T data in the low- or high-temperature region. When the *isotropic* model-free method was chosen, the correlation times were subjected to a constraint with a maximum of 3 ns for global and of 300 ps for effective correlation time during iteration. This method yielded comparable global correlation times with the Arrhenius plot at low temperature, but was divergent from the straight line above 300 K. This behavior can be explained by the nearly full (and at the same time less informative[29f]) NOE close to the extreme narrowing regime and by the smaller separation of the time scales between the global and internal fluctuations at higher temperatures. The "trouble-free" method does not separate global and local motions. Furthermore, it extrapolates the correlation times between extreme temperatures. Therefore it is ideal for deriving the activation energy of reorientation. The measured value for trehalose (E_a = 28.2 kJ/mol) is in good agreement with the data obtained for sucrose[19] since a linear extrapolation to 1.7 M trehalose predicts E_a = 29.9 kJ/mol. The success of the Arrhenius type fit of τ_C suggests that the hydration number[33] of trehalose must be fairly constant in the temperature range of this study and polymerization of the disaccharide cannot play a role at low temperature. An *anisotropic* model-free analysis has also been carried out on the same NOE and T_1 data set using identical upper boundaries for correlation times. We found that the global reorientation of trehalose may be slightly anisotropic in the intermediate temperature regime. In fact, the isotropic and anisotropic error functions and parameter values are nearly identical below 287 K and a similar trend is observed above 337 K. Figure 4a shows the asymmetry parameter A and the τ_1, τ_2 anisotropic global correlation times as a function of temperature. When A = 1 or 0, or $\tau_1 = \tau_2$, the motion may be considered isotropic.[34] If we calculate the moment of inertia for the known average conformation of trehalose we obtain roughly a ratio of 2.9:2.6:1.0 for the principal components. The dominantly isotropic nature of trehalose reorientation suggests heavy hydration of the disaccharide, which is able to mask the

(33) It was shown in ref 4 that the number of unfreezable water molecules in trehalose is eight. It was suggested that this number must be proportional with the number of water molecules in the first hydration shell. For sucrose, for example, 25 water molecules are predicted in the first hydration shell (Engelsen, S. B.; Perez, S. Unpublished theoretical data).

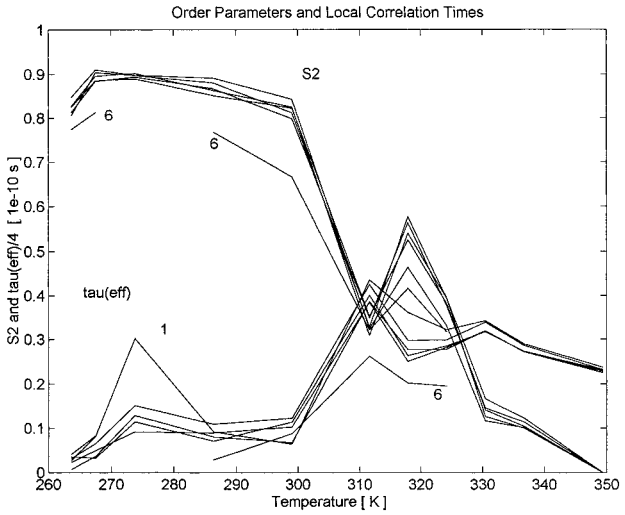

Figure 5. S^2 order parameter and effective correlation times are obtained from the model-free analysis of 5.8/11.7 T data, and plotted against the temperature. Only the C1−H1 and C6−H6 vectors are labeled because they show behavior different from the bulk. Order parameters between 270 and 300 K have a mild slope similarly to published data. Above 300 K it decreases abruptly, but this may happen because the validity of the model-free method is limited in the high-temperature region. However, the surprising fold back of S^2 before freezing could be real. Although effective correlation times suffer from relatively high errors, it can be seen that the importance of local fluctuations is diminished upon cooling.

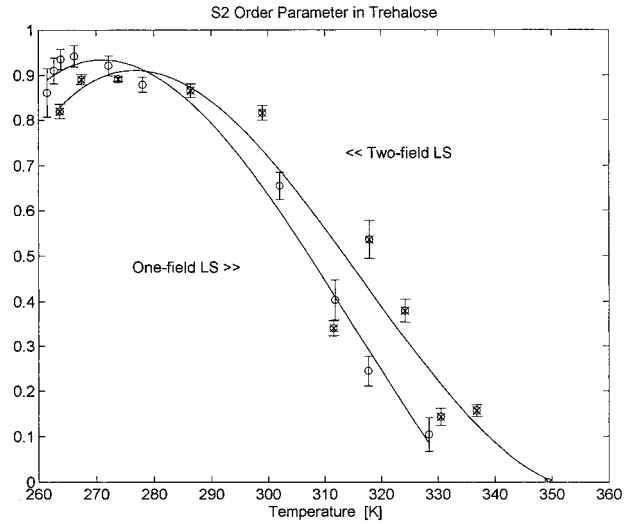

Figure 6. Comparison of two different sets of relaxation measurements accomplished on two slightly different D_2O solutions of trehalose. S^2 order parameters are obtained by the Lipari−Szabo method. Points represent the average of five methine vectors and one standard deviation is labeled with error bars. Points were fitted with third-order polynomial for better visual appearance. "×" labeled points were calculated from 5.8/11.7 T NOE/T_1 data, while "○" labels represent model-free analysis of T_1, T_2, and NOE data measured at 4.7 T field. The similarity of the two curves seems to corroborate the low-temperature disordering in trehalose.

expected anisotropy of its motion. Concerning enhanced anisotropic motion at intermediate temperatures, it is difficult to decide if the anisotropy of motion is enhanced or the Lipari−Szabo method is just less reliable in this motional regime. Figure 4b clearly demonstrates that the separation of the global and local motions is increased more than one order of magnitude below 300 K. This observation allows quantitative interpretation of model-free dynamics below 300 K, a region characteristic for cryogenic properties.[35] Increasing separation of internal and global motions at low temperatures has been predicted and explained theoretically[16,32a] in accordance with the present experimental results. This behavior is a consequence of Kramer's theory and the validity of the Stokes−Einstein−Debye equation. For this reason, increasing separation of local and global motions is not a proof for a hypothetical polymerization of trehalose via hydrogen bonding in the D_2O solution. Long-range ordering or formation of a liquid state crystal is also unlikely under our experimental conditions, since no dipolar couplings were observed in the NMR spectra.

Local Fluctuations. Though there are apparent limitations of the Lipari−Szabo method at elevated temperatures, it is tempting to show data on the whole range of temperature. The temperature dependence of local effective correlation times τ_e and order parameters S^2 are shown on Figure 5. For the hydroxy methyl group not all points were available, but existing data show that the internal fluctuations of the methylene groups are faster if compared to CH vectors, especially at high temperatures. The methine CH vectors show quite similar behavior to each other. Only the C1−H1 internal fluctuations seem to differ from the rest around the freezing temperature of water. We show by error analysis (vide infra) that effective correlation times may suffer from relatively high errors; however, order parameters are well defined for the same species. As it can be seen on Figure 6,[36] a local maximum is observed in the generalized order parameters S^2 between 270 and 280 K when we use the average of five methine parameters in two different series of experiments. The mild slope of the order parameter between 273 and 300 K is comparable to the results observed for monosaccharides[29f] and disaccharides.[29a] We observed a drastic decrease in the order parameters from 300 to 350 K, which is a region rarely studied at high carbohydrate concentration.[29h] Increased spatial fluctuations are not too surprising since elevated temperatures allow higher motional freedom for intramolecular motions. However, in this temperature region the Lipari−Szabo method has limited potential and the results are only qualitative. One of the most fascinating observations of this study is the low-temperature *maximum* in order parameters. We attempt to interpret this strange effect in terms of changes in Gibbs free energy. Originally, Akke et al.[37] introduced a method for determination of the contribution to Gibbs free energy arising from changes in fast intramolecular fluctuations upon binding of small guest molecules to macromolecules. In our case trehalose may have many water molecules in fast exchange between the first hydration shell and the continuum. Therefore two different states of the solution may be characterized by their appropriate temperatures. Such interpretation leads to an extension of Akke's formalism to non-constant temperature.[38] Since we measure the S^2 order parameters at different temperatures, we use the *average temperature* between two points (the difference could be infinitely small). To reveal temperature effects in Gibbs free energy we relate it

(34) For all but the highest temperature point (350 K) the average deviation between the experimental and theoretical NOE and T_1 values is lower than 4%, and in most cases smaller than 2%. Qualitative trends in local correlation times and order parameters were found to be independent of the selection of anisotropic or isotropic model.

(35) We acquired relaxation data at elevated temperatures as well, but when they are evaluated using the Lipari−Szabo method, limitations of that approach must be considered.

(36) Figure 6 also presents control measurements carried out on a similar trehalose solution except that only single field (4.7 T) T_1, T_2, and NOE data were acquired. More details can be found in the error analysis section.

(37) Akke, M.; Brüschweiler, R.; Palmer, A. G. *J. Am. Chem. Soc.* **1993**, *115*, 9832−9833.

(38) Such an extension can be justified. (Akke, M. Personal communication).

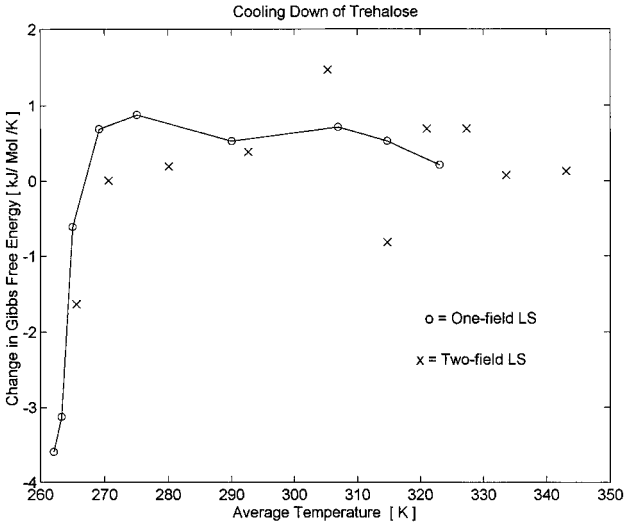

Figure 7. Changes in the Gibbs free energy in trehalose when cooling down of the solution is in progress. In fact, this figure is a different representation of Figure 6. The changes are related to temperature difference between the starting and final temperature. Both experiments show a sudden change in the free energy below 270 K which may explain increased resistance against freezing.

to the difference in temperature between the two states. In this way we arrive at a modification of Akke's equation as follows:

$$\Delta(\Delta G_o)/|\Delta T| = -0.5R(T_1 + T_2)/|T_2 - T_1| \sum \ln[(1 - S^2\mathrm{j},_2)/(1 - S^2\mathrm{j},_1)] \quad (10)$$

We considered contributions arising only from CH fluctuations[39] between two temperatures according to eq 10. Figure 7 was constructed from Figure 6 using eq 10, and is even more characteristic of the cryogenic behavior of the solution, since both of the independent data sets show a sharp cut around the 270 K average temperature point. The drop in Gibbs free energy is much faster when cooling down is in progress if compared to warming up of the solution. The change in Gibbs free energy in the temperature range between 267 and 264 K is at least -1.6 kJ mol^{-1} K^{-1}. If concerted librational motion occurs in the hexapyranose rings, it is reasonable to assume that the C−C, C−O, and O−H vectors have comparable contributions to Gibbs free energy. If this is the case, then there is at least -6 kJ mol^{-1} K^{-1} total free energy change for the trehalose upon cooling below 273 K. This energy may suffice to disrupt local hydrogen bonding. The D_2O solution of trehalose freezes around 261−262 K. However, before freezing, spatial restriction of fast CH fluctuations is diminished and this may help resist a phase transition. Speculation about release of water molecules or reorganization of the hydration shell are difficult until sufficient dynamical calculations including explicit water molecules are carried out.[40] Experimentally, a microcalorimetry study could help to clarify the source of increased CH fluctuations. However, such study is out of the scope of the present work.

Error Analysis of Model-Free Dynamics. We have acquired two independent data sets with two slightly different D_2O solutions (1.7 M) of trehalose. It can be seen on Figure 6 that two S^2 curves derived from the Lipari−Szabo analysis (T_1 and NOE data at 11.7 and 5.8 T for the first and T_1, T_2, and NOE measured at 4.7 T for the second) have quite similar appearances. The error bars of this figure show the scatter of order parameters for the five individual CH vectors in the molecule. However, neither accidental small scatter of the derived parameters nor the good agreement between experimental and theoretical relaxation parameters (1−2% deviation below 286 K, and less than 4% for the whole temperature range) warrants low error limits for order parameters or effective correlation times. Because of the non-linear nature of the problem we carried out Monte-Carlo error analysis of the experiments.

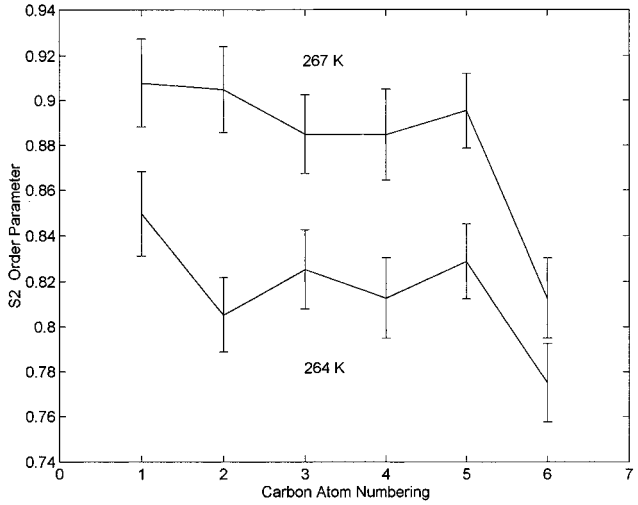

Figure 8. Representative Monte-Carlo error analysis of the model-free fit of relaxation data at 264 and 267 K. 250 artificial T_1 and NOE data were generated by addition of random Gaussian noise to original data. 1 and 2% noise were applied according to the errors in T_1 and NOE. Error bars for S^2 represent the 90% confidence limit. Apparently, the difference in order parameters between CH and CH_2 groups is significant. The difference between the two curves is also significant statistically.

Figure 8 shows a comparison of S^2 order parameters measured in the low-temperature range, at 267 and 264 K from 11.7/5.8 T relaxation experiments. Error bars for S^2_i represent the *90% confidence interval*. It can be seen that the CH_2 group shows increased mobility with respect to CH vectors at both temperatures. More importantly, *the 0.05−0.1 drop in all S^2 parameters upon cooling is statistically significant* (e.g. for the 2-CH vector S^2_2 decreased from 0.90(0.02) to 0.81(0.02)). For the same data set effective correlation times are often ill defined (50−100% errors), which is not unprecedented in the literature. The global correlation times were $\tau = 2.13(0.05)$ and 2.24(0.05) ns at the two temperatures. When relaxation data (T_1, T_2, and NOE) measured at 4.7 T were analyzed, we had higher error limits. For the data set yielding $\tau = 2.19(0.12)$ ns correlation time $S^2_2 = 0.95(0.06)$ was found for the 2-CH vector. At a temperature of two degrees colder (just before freezing) this value dropped to 0.86(0.03).[41] This might not seem to be a convincing difference at first glance, but a 0.05−0.1 drop is observed again for *all* CH vectors upon cooling.

Error analysis of the model-free data of two independent series of measurements seems to support the observation that the order parameters of trehalose may decrease before the D_2O solution freezes. A third independent measurement (obtained from T_1, T_2, and NOE data at 11.76 T) not presented here also demonstrated a drop in order parameters upon cooling.

(39) CH_2 is excluded since some data were unavailable and other fluctuations, e.g. OH groups, cannot be measured by this method.

(40) In a molecular dynamics simulation study—with both pyranose rings kept rigid—it was suggested that trehalose function against water stress is probably not due to the modification of the properties of water. Necessarily, this theoretical work is unable to consider ring librational dynamics in trehalose. Donnamaria, M. C.; Howard, E. I.; Grigera, J. R. *J. Chem. Soc., Faraday. Trans.* **1994**, *90*, 2731−2735.

(41) See Supporting Information for Monte Carlo error analysis of T_1 and individual model-free parameters.

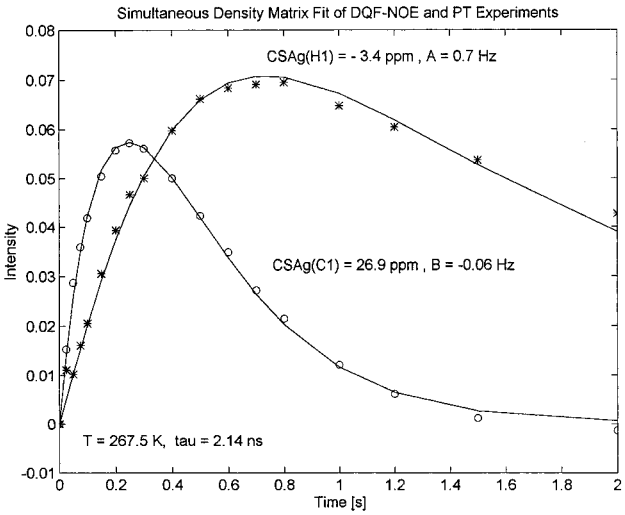

Figure 9. Simultaneous fit of the ^{1}H and ^{13}C CSA CSA/DD interference measurements according to Farrar's method. In fact, this applies the Redfield relaxation matrix picture for two spins. "*A*" and "*B*" represent random field terms for ^{1}H and ^{13}C, and the small negative value for *B* may be an indication of the limits of the two-spin approach. However, there is a fairly good agreement between the much simpler initial rate method (applied throughout this work) and the Farrar method.

Proton and Carbon Chemical Shift Anisotropy. Liquid state measurement of CSA at natural abundance is generally a difficult task. The measured CSA/DD interference terms in longitudinal relaxation are small and they are strongly influenced by molecular dynamics. For the simplest isotropic reorientation model (eqs 4 and 5), it can be shown that the most sensitive region for both nuclei is between 0.2 and 2 ns at the applied NMR field (11.76 T). In this study the experimental cross-correlated relaxation rates for ^{1}H and ^{13}C CSA_g factors were obtained from the initial slope of DQ-filtered transient heteronuclear NOE or polarization transfer enhanced $\langle S_zI_z\rangle$ to $\langle I_z\rangle$ buildup curves as described in our previous work.[8]

Figure 9 shows the buildup curves measured at 267 K for H1 and C1 CSA. In some particular cases including this, in addition to the initial rate approach, a Redfield relaxation matrix fit was applied according to the work of Farrar[12t] et al. We found that in case of sufficient signal to noise ratio and careful experimental setup the results are virtually identical using either two-spin approach. Cross-correlated relaxation arising from carbon CSA could be easily detected at low temperature since the global correlation time (2.13 ns) is close to optimum. The sensitivity for ^{1}H CSA detection is optimal approximately at $\tau_C = 0.3$ ns, but the sensitivity is still acceptable at low temperatures because the inverted proton magnetization is sizable in the DQF-NOE experiment.

By using the isotropic global correlation times derived from the "trouble-free" approach, experimental cross-correlated relaxation rates could be well fitted (assuming constant ^{13}C or ^{1}H CSA_g over the entire temperature range) against correlation times. Figure 10 shows this fit for C1, and predicts 27.8 ppm for the CSA_g value. The success of this fit nicely demonstrates the applicability of the "trouble-free" approach and the simplest cross-correlated spectral density function (eqs 4 and 5).

In order to clarify if some shift anisotropies are temperature dependent and/or may be influenced by the fast intramolecular fluctuations, we interpreted the measured cross-correlated relaxation rates with both the isotropic (eq 9) and the anisotropic forms of the model-free approach and compared the results. Figures 11a and 11b show these comparisons for ^{13}C and ^{1}H CSA_g. There is virtually no difference between the CSA_g values obtained by either isotropic or anisotropic dynamics. Carbon

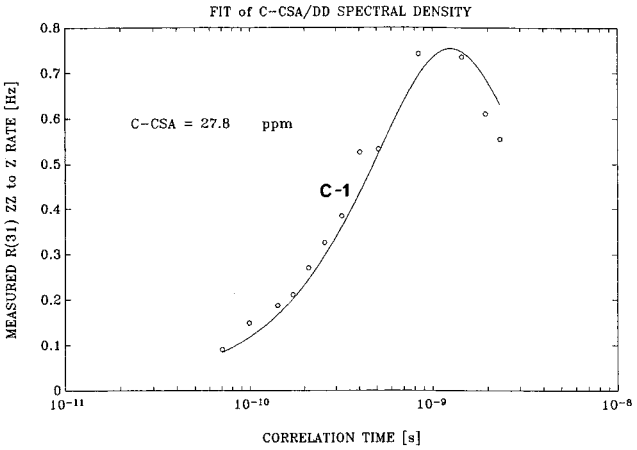

Figure 10. Fit of $\langle zz\rangle$ to $\langle z\rangle$ DD/CSA cross-correlated relaxation rates of ^{13}C-1 against global correlation times yields CSA_g for C1. The success of the fit over the entire temperature range is an indication of the reliability of "trouble-free" correlation times and the validity of the initial rate method.

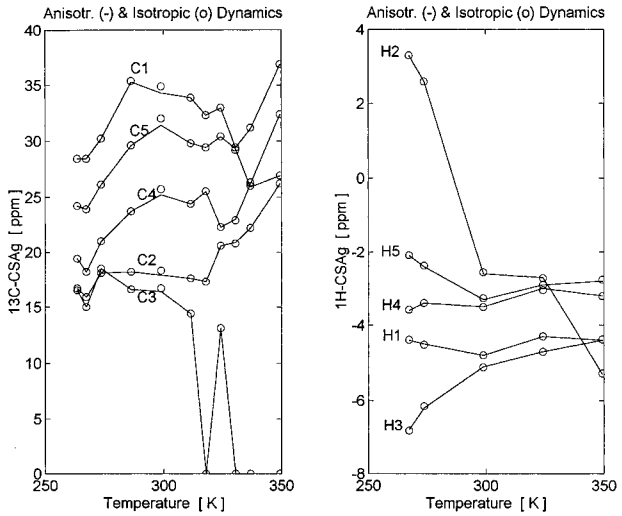

Figure 11. Temperature dependence of ^{1}H and ^{13}C CSA_g factors in α,α-D-trehalose. Comparison of isotropic and anisotropic Lipari−Szabo evaluation shows virtually no difference in shift anisotropies. All anisotropies are smooth functions of temperature, and the changes are close to the probable error limits of the method. It has been proved that strong couplings seriously distort CSA data as it has been found at positions H2/C2 and H3/C3.

and proton shift anisotropies at positions 1, 4, and 5 are smooth functions of temperature and may be considered nearly constant within experimental errors. This finding is somewhat surprising since applicability of the model-free method is limited in those regions where global and internal fluctuations occur on the same time scale. Interestingly, the C-1 anisotropy at low temperature (28 ppm) is nearly coincident with the value obtained by the "trouble-free" dynamics. Since this latter method disregards local fluctuations, the low-temperature agreement must be a consequence of negligible fast fluctuations at subzero temperatures. These experimental results suggest, that in our case, omission of local fluctuations from relevant spectral densities may lead to underestimation of CSA-s by ca. 5−20%.

The chemical shift separation of the anomeric proton from the bulk of the ^{1}H NMR spectrum warrants that second-order effects (ABX strong coupling pattern in the ^{13}C satellite spectrum) are absent for H-1 and C-1. However, depending on the applied magnetic field, any other signal might be affected, as it is well-known from the NMR of carbohydrates. Even a small distortion of a CH doublet can lead to annoying interfer-

Table 1. Comparison of ^{13}C and ^{1}H CSA_g Values [ppm] in Normal and [2,4,6-^{2}D] Trehalose[a]

	deuteriotrehalose		normal trehalose	
		$T = 302$ (±3) K		
H1	−4.0	−4.1	−4.8	
H3	−2.6	−3.3	−5.1	
H5	−2.7	−3.0	−3.3	
		$T = 320$ (±3) K		
H1	−3.7	−3.8	−4.3	−3.5
H3	−2.6	−2.5	−4.7	−4.3
H5	−2.3	−3.1	−2.9	−2.7
C1	+32		+33	+29
C3	+23		+13	0
C5	+31		+30	+24

[a] When two values are given, it means two independent measurements.

ence with cross-correlated relaxation, since they are manifested in asymmetric multiplet relaxation. Apparent CSA_g factors shown on Figure 11 would suggest that H-2, H-3 and C-2, C-3 shift anisotropies are seriously affected by the temperature. If such effects appear for vicinal proton pairs, strong coupling is always suspected since the applied pulse sequences measure multiplet asymmetries. The simplest experimental way for ruling out strong coupling[42] is to run a 2D HETCOR experiment. If a pair of vicinal protons H_A and H_B have resolved coupling and the carbon satellite of H_A closely overlaps with H_B, then carbon C_A exhibits a cross peak not only to H_A, but a smaller one to H_B as well. The 2D HETCOR spectrum of trehalose acquired at 11.76 T clearly demonstrated that this was the case for C-2(C-3),H-2,H-3. Figure 11 shows that strong coupling can increase or decrease the value and even change the sign of the apparent CSA_g term, in a hardly predictable manner. For this reason, the temperature-dependent CSA effects observed at positions 2 and 3 are most probably attributed to strong coupling effect. This may be caused by tiny, temperature-induced changes in differences between the isotropic shifts of the H-2 and H-3 protons. Such strong coupling effects can be removed in carbohydrates by deuteration at alternating positions of skeleton CH's. For this reason we prepared the 2,4,6-deuteriotrehalose.[43] Two independent sets of CSA data were acquired for both normal and deuterated trehalose at 302(3) and 320(3) K. The CSA_g data are presented in Table 1. Apparent CSA_g values clearly show that at positions 1 and 5 the proton and carbon shift anisotropies are independent of deuteration, but a factor of 2 difference is observed at position 3, which is affected by strong coupling with H2 in normal trehalose. Based on this observation, the values measured in deuteriotrehalose can be accepted, which gives on average −2.8 ppm for H3 and 23 ppm for C3 CSA_g in this temperature range. The apparent CSA_g values found for H2 and C2 (Figure 11) have no physical meaning since they are influenced by strong coupling.

In summary, we did not observe dramatic changes in shift anisotropies in this temperature-dependent ^{1}H and ^{13}C CSA study. Slight, continuous changes seem to occur; however, these are close to the error limits of the applied methods. On the other hand, the methods tested here allow the measurement of geometry-dependent CSA_g terms of carbohydrates in a broad dynamical range.[44]

Conclusions and Open Questions

We have developed and applied new NMR techniques in order to determine geometry-dependent proton and carbon chemical shift anisotropies in solution. Monitoring the temperature dependence of small anisotropies in carbohydrates is demanding because the dynamics of the system is also changing. This study proves that if a large dynamic range is spanned by molecular motions, both isotropic and anisotropic model-free dynamics may be suitable for CSA study. The simple "trouble-free" dynamics gives access to global correlation times in a broad temperature range and is useful for deriving CSA_g values.

^{1}H and ^{13}C chemical shift anisotropies in trehalose change smoothly in the entire temperature range, in accordance with the fairly stable average conformation of trehalose. Strong coupling effects in apparent CSA_g factors revealed temperature dependence of isotropic chemical shift difference between H2 and H3. A challenging question is if the observed small changes are related to changes in the hydrogen bonding network of trehalose in the aqueous media.

Concerning the structure of trehalose in dilute solution, we were able to verify by NMR measurements that the preferred conformation of the interglycosidic bond is remarkably stable over a large temperature range. This finding is in agreement with previous molecular mechanics calculations and can have important consequences for the cryogenic qualities of trehalose in stabilizing the lipid bilayer membranes of phospholipids.

Evaluation of the relaxation data of a highly concentrated solution of trehalose led to interesting observations. Increasing separation of local and global motions upon cooling allows the application of model-free dynamics for a small molecule the size of trehalose. Thermodynamic interpretation of the order parameters shows a maximum in change of Gibbs free energy below the freezing point of water. This may suggest that internal fluctuations are increasing in trehalose as the temperature of the D_2O solution falls below 0 °C. One possible explanation of these findings may be that the small differences in hydrogen bonding energies between coordinated water molecules and the equatorial hydroxyl groups of trehalose are more pronounced at low temperature. Therefore the temperature change may selectively promote or break specific hydrogen bonding interactions. If it is so, the resistance of the coordinated water molecules against the freezing could be tentatively explained by restructuring of the hydration sphere around the trehalose. Perhaps microcalorimetric studies could reveal more details on disordering in trehalose upon cooling.

Experimental Section

Preparation of [1-^{13}C]Trehalose. The glycosyl acceptor [1-^{13}C]-2,3,4,6-tetra-*O*-benzyl-D-glucose (**1**) and the glycosyl donor *O*-(2,3,4,6-tetra-*O*-benzyl-*β*-D-glucopyranosyl)trichloroacetimidate (**2***β*) were prepared from [1-^{13}C]-D-glucose and D-glucose.[45] From these precursors the per-*O*-benzylated trehalose derivatives **3**α,α and **3**α,*β* could be prepared with 74% yield (α,α:α,*β* = 2:1) via the trichloroacetimidate glycosylation method.[46] Hydrogenation of **3**α,α afforded the asymmetrically ^{13}C-labeled trehalose **4**α,α.

[1-^{13}C]-2,3,4,6-Tetra-*O*-benzyl-α-D-glucopyranosyl-(1→1)-2′,3′,4′,6′-tetra-*O*-benzyl-α- (3α,α) and *β*-D-glucopyranoside (3α,*β*). Compounds **2***β* (0.5 g, 0.72 mmol) and **1** (0.39 g, 0.72 mmol) were dissolved in 20 mL of dry ethyl ether at room temperature. The reaction mixture

(42) Kövér, K. E.; Mádi, Z.; Batta, Gy. *Magn. Reson. Chem.* **1991**, *29*, 619−624.

(43) In the ^{1}H NMR spectrum of 2,4,6-deuteriotrehalose three broad singlets were detected at 5.10 (H-1), 3.76 (H-3), 3.72 (H-5) ppm while the assignment of the ^{13}C NMR spectrum is 94.30 (CH-1), 73.59 (CH-3), 73.13/73.08 ppm (split signal for CH-5 caused by incomplete deuteration at C-6) and broad signals 71.77 (CD-2), 70.43 (CD-4), 61.41 (CD_2-6) ppm. The carbon shifts at deuterated positions were ca. 0.25−0.3 ppm upfield shifted with respect to normal trehalose.

(44) Solvent and temperature dependence of solution-phase ^{1}H and ^{15}N CSA in protected amino acids revealed that CSA may be a sensitive probe of H-bonding and solvation. Kövér, K. E.; Batta, Gy.; Gervay J.; Hruby, V. 13th European Experimental N.M.R. Conference, May 19−24, 1996, Paris, Abstract p 23.

(45) Glaudemans, C. P. J.; Fletcher, H. G., Jr. *Meth. Carbohydr. Chem.* **1972**, *5*, 373. Schmidt, R. R.; Mitchel, J. *Tetrahedron Lett.* **1984**, *25*, 821.

(46) Wegmann, B.; Schmidt, R. R. *J. Carbohydr. Chem.* **1992**, *11*, 255.

was cooled to −10 °C and trimethylsilyl triflate (0.06 mL, 0.3 mmol) was added. After 1.5 h the reaction mixture was treated with excess solid sodium hydrogen carbonate and then with ethyl ether/sodium hydrogen carbonate solution in water. The ethyl ether extract was washed with water, dried with sodium sulfate, and then concentrated. The oily residue was chromatographed on silica gel (chloroform/ethyl ether = 24:1) affording **3**α,α (0.39 g, 51%) and **3**α,*β* (0.19 g, 25%) as an oil.

3α,α$[\alpha]^{20}_D$: +81° (*c* 1, $CHCl_3$) (lit.[47] $[\alpha]^{20}_D$ +83° (*c* 1.6, $CHCl_3$)). Anal. Calcd for $C^*_{68}H_{70}O_{11}$: C, 76.90; H, 6.63. Found: C, 76.26; H, 6.49.

3α,*β*$[\alpha]^{20}_D$: +41° (*c* 1.4, $CHCl_3$) (lit.[44] $[\alpha]^{20}_D$ +43° (*c* 1.35, $CHCl_3$)). Anal. Calcd for $C^*_{68}H_{70}O_{11}$: C, 76.90; H, 6.63. Found: C, 76.38; H, 6.52.

[1-^{13}C]-α-D-Glucopyranosyl-(1→1)-α-D-glucopyranoside (4α,α). Compound **3**α,α (370 mg, 0.34 mmol) was dissolved in 10 mL of dry ethyl acetate and 10 mL of dry methanol. It was than hydrogenated in the presence of 150 mg of palladium on carbon. After 3 h the reaction mixture was filtered and the solution was concentrated to dryness. The residue was recrystallized from aqueous ethanol yielding **4**α,α (0.128 g, 98%) as the dihydrate. Mp 98−100 °C; $[\alpha]^{20}_D$ +176° (*c* 1.5, H_2O) (lit.[48] mp 97−98 °C $[\alpha]^{20}_D$ +178° (*c* 2, H_2O)).

Preparation of [2,4,6,6′-^{2}H]-α,α-Trehalose. A Raney nickel/deuterium oxide slurry was prepared by decanting Raney nickel slurry (Aldrich: 50% slurry on water) and washing the catalyst with deuterium oxide thrice. The catalyst was resuspended in an equivalent amount of deuterium oxide so as to have a 50% slurry. α,α-D-Trehalose dihydrate (1g, 2.6 mmol) was dissolved in 15 mL of D_2O before adding 7 mL of Raney nickel slurry. The reaction was refluxed for 4 h before being cooled to 20 °C. The pure sugar was isolated by filtering off the catalyst followed by lyophilization.[49]

For the purpose of the determination of long-range interglycosidic carbon−proton coupling constants, 10 mg of [1-^{13}C]trehalose (lyophilized 3 times from D_2O) was dissolved in 500 μL of D_2O and placed in a 5 mm NMR tube. $^3J_{COCH}$ couplings were obtained from ^{1}H coupled ^{13}C spectra using UNITY 300 and DRX 500 spectrometers.

A 1.7 M D_2O solution of α,α-trehalose (SIGMA) was prepared after repeated lyophilization (3 times) from D_2O solution. Two milliliters of this solution was loaded into a 10 mm NMR tube without oxygen depletion. This concentration was close to saturation in the temperature range of 264−350 K. CSA data were accumulated at 11.75 T field, and NOEF and ^{13}C T_1 data were obtained at 11.75 and 5.87 T magnetic fields with Bruker AM or at 4.7 T with WP spectrometers for T_1, T_2, and NOEF. Temperatures were calibrated either with 100% methanol (below 300 K) or ethylene glycol. The accuracy of temperature calibration is ±2 K, and the reproducibility is believed to be ±1 K.

^{13}C T_1 values were obtained with standard inversion recovery experiments under composite pulse proton decoupling, and 20−25 items were used as the variable delay list. Generally 10 T_1 relaxation delays were allowed before the inversion pulse. Typically 16−32 scans were accumulated for each point, and the FID's were weighted with matched exponential functions and zero filled. After Fourier-transformation an automatic 4th order polynomial baseline correction was applied to the spectra. The recovery curves were evaluated using a three-parameter single-exponential fit. Built-in spectrometer routines gave identical values for T_1 as a MATLAB[50] application. For measurement of the ^{13}C−{^{1}H} NOEF values, the total number of scans of the difference experiment were comparable to the total number of scans in the T_1 experiments. To avoid temperature drift effects the NOE and T_1 measurements were interleaved. The processing for NOE was done similarly as for T_1 spectra and the amplitude of difference signals were compared to the reference spectrum. T_2 relaxation times at 4.7 T were measured using the 1D method starting with INEPT preparation. During relaxation in the XY plane a CPMG sequence composed from hard ^{13}C 180° pulses at every 200 μs was applied.[51] Signal to noise ratios were determined from the original T_1, T_2, and NOE spectra. Then a noise of normal distribution was added to the measured intensities to yield an identical S/N ratio. T_1 and T_2 error limits were derived from at least 250 randomized data sets within the 90% confidence limit. Typical relative errors were less than 1% and 2% for T_1 and NOEF, respectively. T_2 errors at 4.7 T field were found between 2 and 3%. Repeated measurements for relaxation data were consistent with these error ranges. Cross-relaxation rates in C−H vectors were obtained from eq 7 and the isotropic correlation times were derived using eq 8. Error target functions for the Lipari−Szabo analysis[9] were compiled as given by Dellwo and Wand.[10] The global correlation time τ_c and local S^2 order parameters and τ_e effective correlation times were fitted simultaneously using the *constr* optimization routine of MATLAB. For the maximum of the τ_c and τ_e, upper boundaries of 3×10^{-9} and 3×10^{-10} s were allowed. An additional constraint of $\tau_1 > \tau_2$ was maintained for fitting the anisotropic model. For the purpose of Monte-Carlo error estimation, the relaxation data were randomized with Gaussian noise 250 times within their error limits, and then fitted repeatedly for the model-free parameters.

Cross-correlated relaxation rates for ^{1}H-CSA_g were obtained from the buildup rate of DQ-filtered transient heteronuclear NOE according to published pulse sequences.[8] Variable delay lists with 17−18 items were used up to 2−5 ^{13}C T_1 values. For ^{13}C-CSA_g determination the polarization-transfer enhanced sequence was employed.[8] The INEPT $^1/_4J$ delay was set to 1.6 ms. The random ^{1}H spin-lock field was applied at full power for 3 ms with ±50% randomization in order to filter out unwanted in-phase carbon polarization. A composite ^{1}H-decoupling scheme was applied at the lowest possible power during acquisition. Similarly to the ^{1}H-CSA_g experiments data accumulation lasted from a couple of hours to overnight. The 90° ^{13}C and ^{1}H pulses for the 10 mm probeheads were 13 and 44 μs at 11.75 T, and 11 and 40 μs at 5.87 T field, respectively. The appropriate pulses for the 5 mm probehead at 4.7 T were 9 and 28 μs. The cross-correlated relaxation rates were determined from the initial slope of the buildup curves after a double exponential fitting of the entire curve. The analytical first derivative at zero delay gave the buildup rate. All calculations were carried out using the MATLAB software package.

Acknowledgment is made to the donors of The Petroleum Research Fund, administered by the American Chemical Society, and The State of Arizona Materials Characterization Program for partial support of this research. Gy.B. and K.E.K. gratefully acknowledge the Hungarian grants OTKA 1144 and T-014982 for generous support and OTKA, OMFB, and Phare Accord equipment grants for the purchase of a DRX 500 spectrometer. We are also grateful to Professor Michael Barfield, Professor Michael Brown, and Dr. Paul Marchetti for their helpful discussions. Computer facilities were provided by the University of Arizona Computer Graphics Facility and Professor Michael F. Brown.

Supporting Information Available: Seven tables containing T_1 and NOE data at 11.76 and 5.87 T fields, model-free parameters equipped with Monte-Carlo error analysis for the same data are presented and Gibbs free energy data for 11.76/5.87 and 4.7 T measurements as well; figures show T_1 fit with error determination, Monte-Carlo error analysis of model free data at 267 K, and strong coupling effects in the HETCOR spectrum; applied anisotropic spectral density function and dipolar T_1, T_2, and NOEF expressions are also given (10 pages). See any current masthead page for ordering and Internet access instructions.

JA962807Q

(47) Pavia, A. A.; Rocheville, J. M.; Ung, S. N. *Carbohydr. Res.* **1980**, *79*, 79.

(48) Lemieux, R. U.; Bauer, H. F. *Can. J. Chem.* **1954**, *32*, 340. Stewart, L. C.; Richtmyer, N. K.; Hudson, C. S. *J. Am. Chem. Soc.* **1950**, *72*, 2059.

(49) Although this compound has been reported in the literature, previous reports showed that more than 70% of 3-hydrido exchange occurred. By performing the reaction at reflux for only 4 h exchange at C-3 could be avoided. Abbate, S.; Giuseppina, C.; Naffi, A. *Carbohydr. Res.* **1991**, *210*, 1−12.

(50) MATLAB Reference Guide. Math Works, Natick, MA, 1992.

(51) Kowalewski, J.; Morris, G. A. *J. Magn. Reson.* **1982**, *47*, 331. Kay, L. E.; Nicholson, L. K.; Delaglio, F.; Bax, A.; Torchia, D. A. *J. Magn. Reson.* **1992**, *97*, 359. Palmer, A. G., III; Skelton, N. J.; Chazin, W. J.; Wright, P. E.; Rance, M. *Mol. Phys.* **1992**, *75*, 699.